



# Measurement of jet substructure observables using the ATLAS detector.

Iain Bertram  
Lancaster University  
Monday 15 July  
QCD@LHC2019

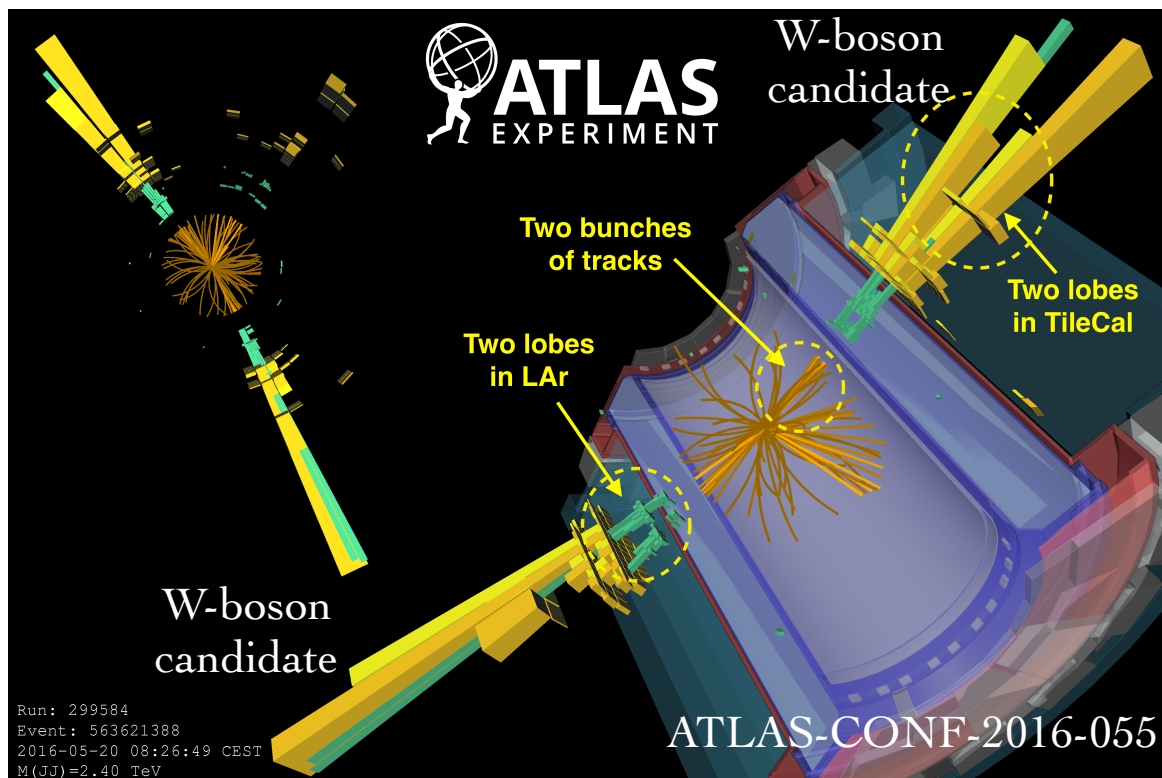
- The internal structure of jets can be used to

- study QCD
- distinguish the origin of jets between light quarks, gluons and hadronic decays of heavy particles (W, Z, H or top quark)

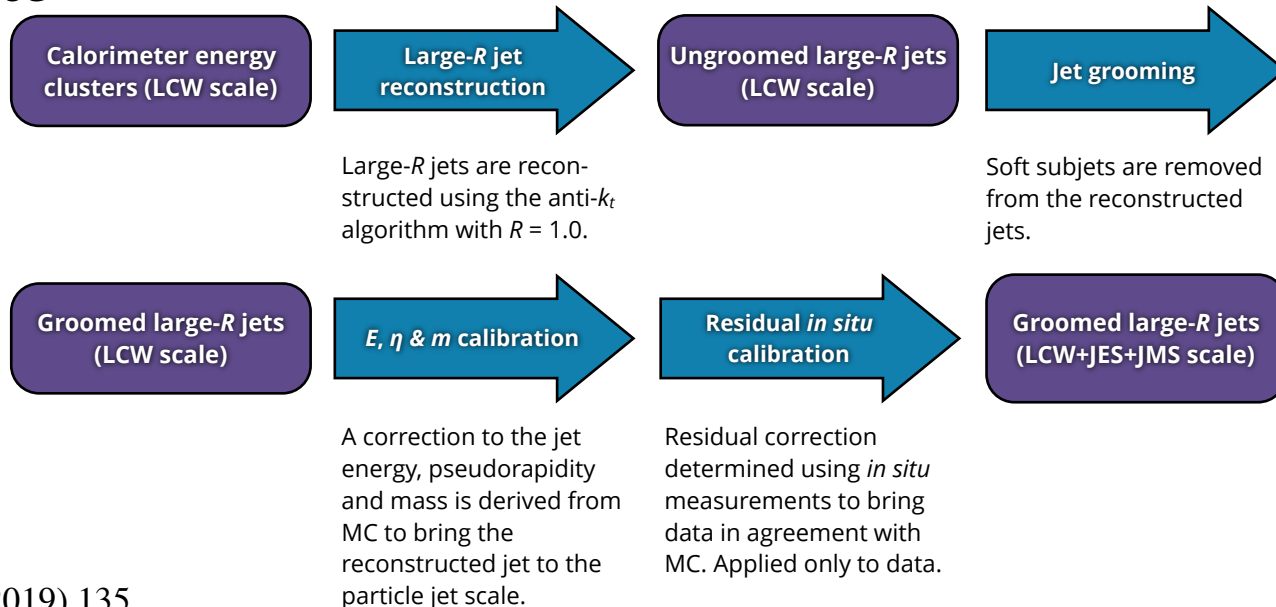
- Many types of jets used in ATLAS

- calorimeter-based, particle-flow, track-based
- radius  $R = 1.0, 0.8, 0.4, 0.2$ , variable- $R$

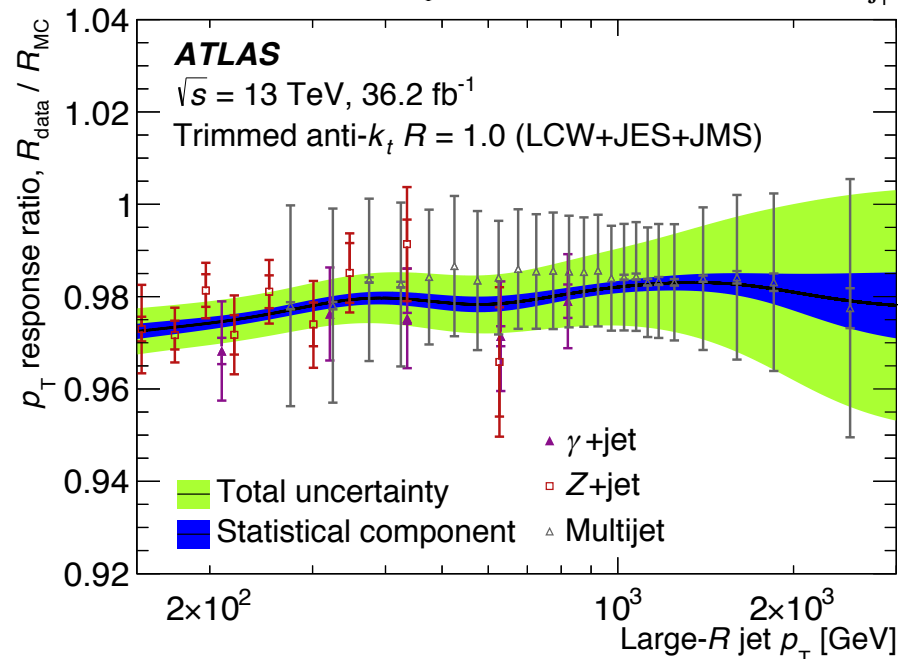
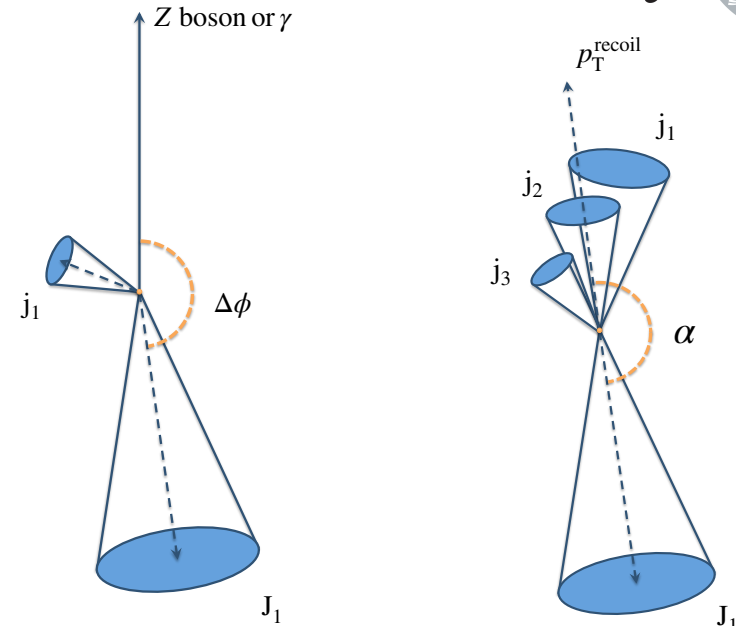
- Calorimeter-based  $R = 0.8$  and  $1.0$  jets reconstructed with anti- $k_T$  algorithm are used for the substructure results presented here.



- Calorimeter jets are built from topological clusters (representing particle deposition)
  - start with a cell  $4\sigma$  above noise and add neighbouring cells  $2\sigma$  above noise and the surrounding layer
  - splitting algorithm separates nearby clusters
  - clusters are calibrated based on properties related to shower development (Local Cluster Weighting)
  - clusters are combined into jets using the anti- $k_T$  algorithm
- Trimming:** removes  $R = 0.2$  subjets with  $p_T < 5\%$  of jet  $p_T$ , to reduce pile-up dependence

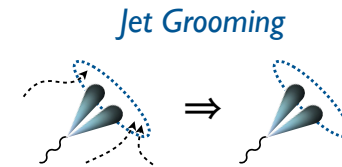


- In situ calibration uses “balancing” with well-measured objects: photons,  $Z \rightarrow ll$ , small-R jets
- $p_T$ -dependent scale factors are derived to rescale the jet 4-momentum
- provides systematic uncertainties on the jet energy scale - “**top-bottom**” approach
- Average correction
  - no access to differential quantities



- uncertainties are computed from the topological clusters and propagated to the jet substructure observables (“**bottom-up**” approach):
  - isolated calorimeter cell clusters are matched to tracks: the mean and the standard deviation of  $E/p$  is used for the cluster energy scale and resolution uncertainties; the standard deviation of the relative position is used for the angular resolution uncertainty
  - the reconstruction efficiency uncertainty is evaluated from the fraction of tracks without a matched cluster.
  - Uncertainties are also applied to account for:
    - energy correlations between the clusters
    - fraction of hadrons that are not pions
    - effect of cluster splitting and merging
- Uncertainties from calorimeter/track ratios are of the same size (can only be measured for average quantities)

- The Trimming procedure is not analytically calculable
  - trimmed jet measurements can only be compared to the NLL predictions
- The soft-drop procedure allows comparison to NLO+NLL and LO+NNLL predictions for the jet mass
  - clusters jet constituents with Cambridge-Aachen algorithm and retraces the clustering history from the last branching

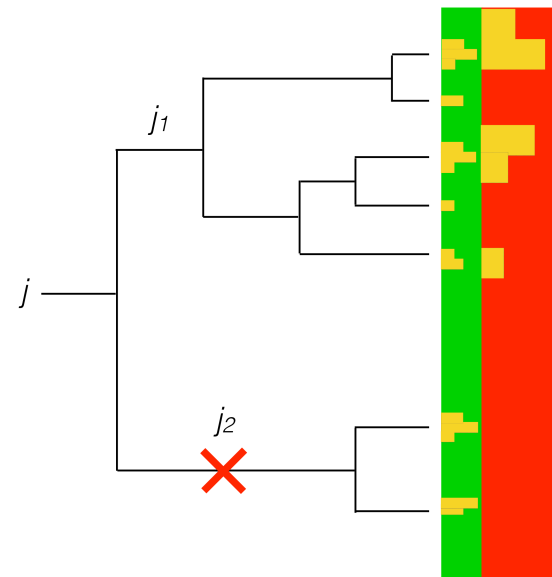


- consider a jet of radius  $R$  with only two constituents.

The soft-drop procedure removes the softer component unless

$$\frac{\min(p_{T,j_1}, p_{T,j_2})}{p_{T,j_1} + p_{T,j_2}} > z_{\text{cut}} \left( \frac{\Delta R_{12}}{R} \right)^\beta,$$

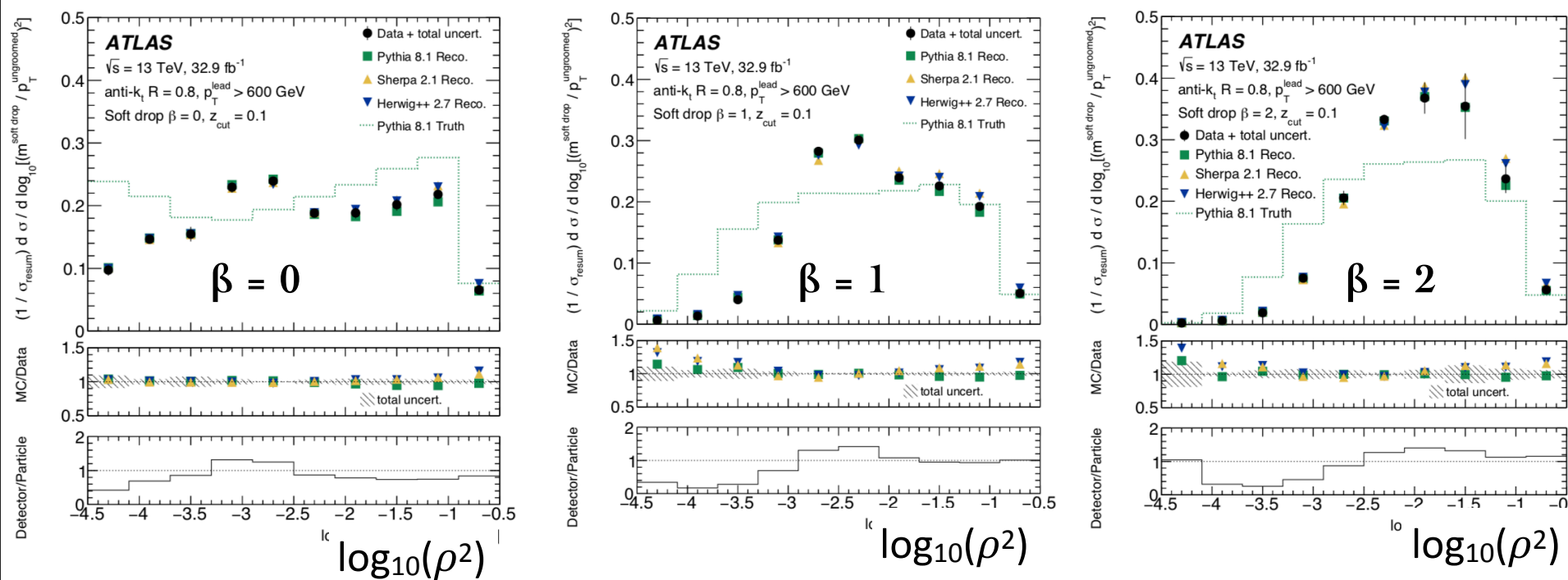
- $z_{\text{cut}}$  is the soft-drop threshold
- $\beta$  is angular exponent ( $\beta \rightarrow \text{infinity}$ : ungroomed jet)



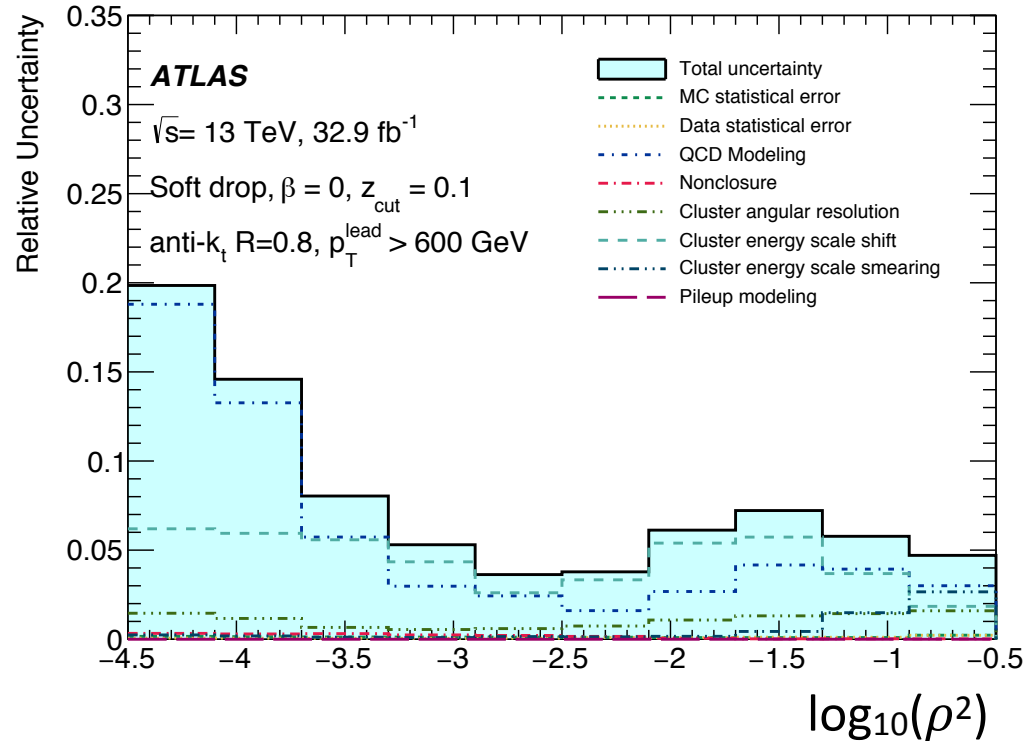
# Soft-drop Jet Mass

- Ungroomed dijet events with radius  $R=0.8$ .
  - Leading jet  $p_T > 600$  GeV
  - two leading jets have similar  $p_T$ :  $p_{T,1} / p_{T,2} < 1.5$

- To reduce  $p_T$  dependence we examine:  $\rho = m^{\text{soft drop}} / p_T^{\text{ungroomed}}$



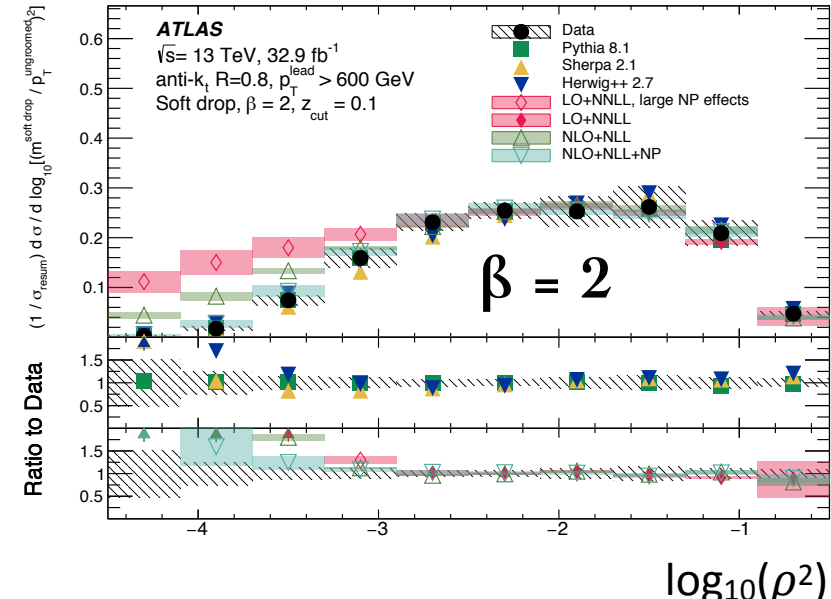
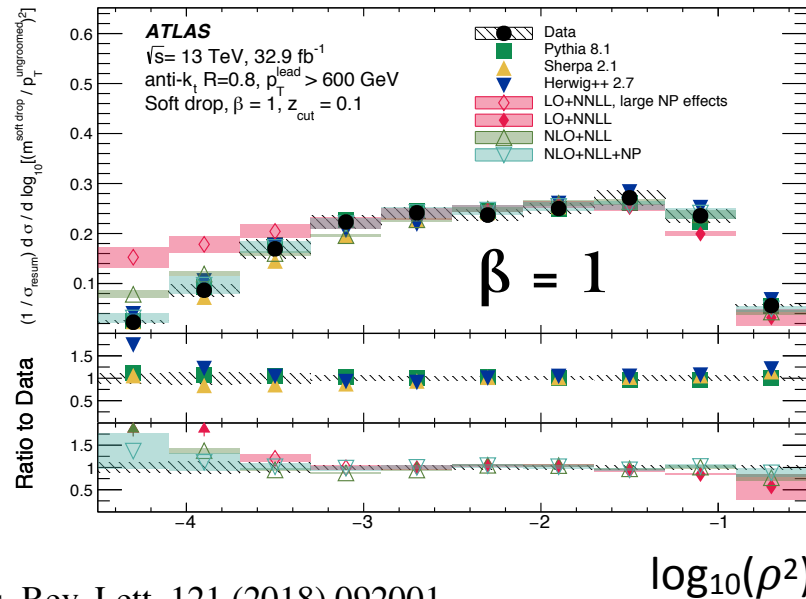
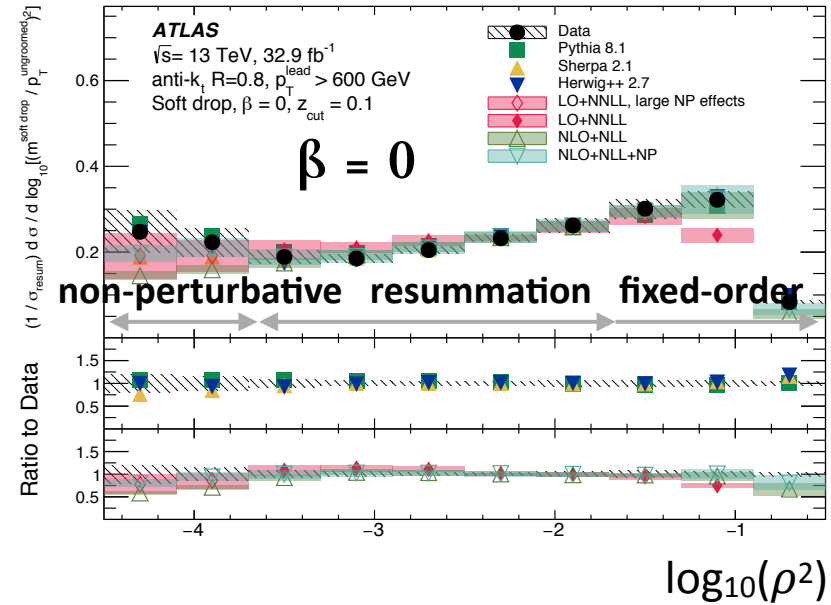
- Data compared with reconstructed Pythia, Sherpa and Herwig simulations and truth-level Pythia.



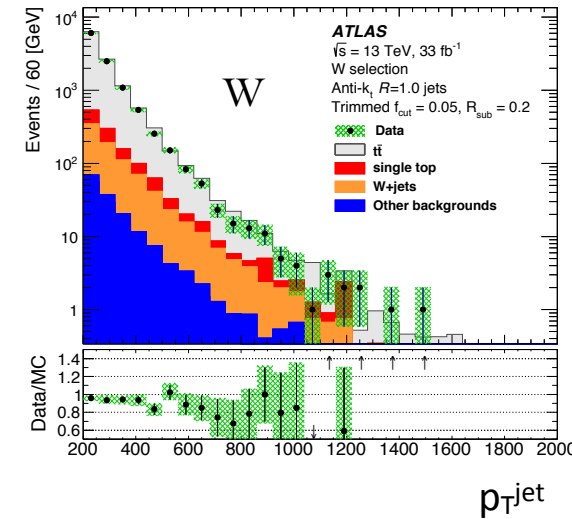
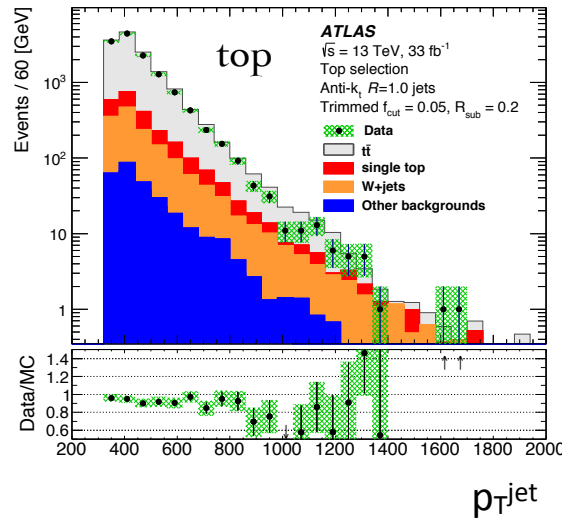
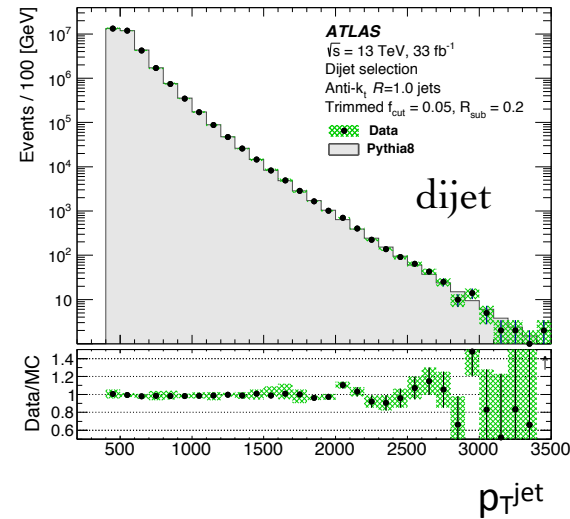
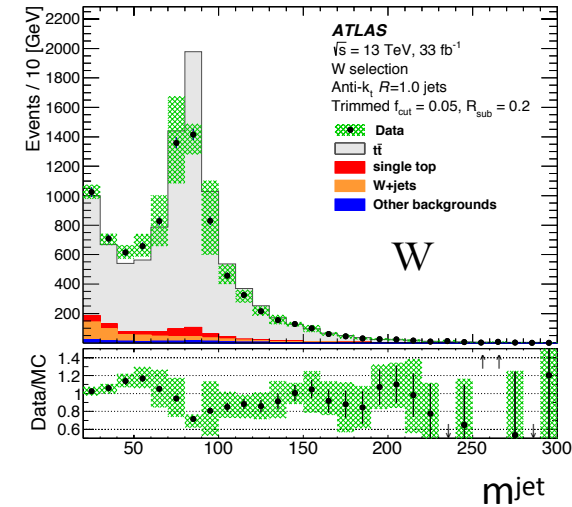
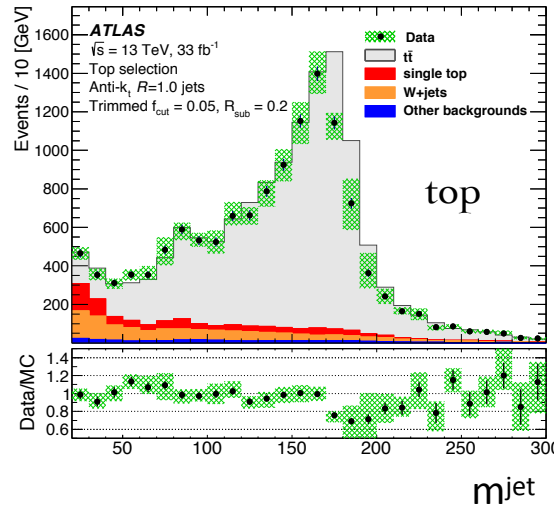
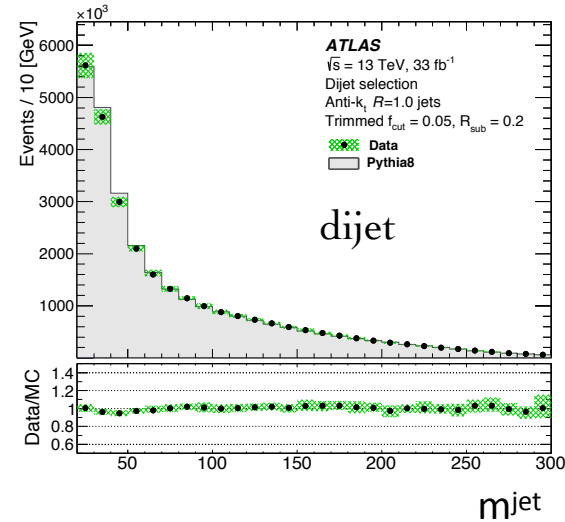
- Dominant Uncertainties
  - QCD Modelling: Pythia 8.186 vs Sherpa 2.1.1 (Herwig++ 2.7.1 produces uncertainties of the same order)
  - calorimeter cluster energy scale shift (smearing) at low (high)  $\rho$



- Mostly good agreement with generator predictions
  - The exception is at low values of  $\rho$
  - To get good agreement requires LO+NNLL with large non-perturbative corrections.



- Two Data sets:
  - dijet: two large  $R=1$  calorimeter jets
  - semileptonic tt: leptonic top and top-quark large- $R$  jet or W-boson large- $R$  jet
- Selection uses trimmed jets.
  - measurements made for both trimmed and soft-drop jets.
- Measure many different observables
  - relevant for W/top tagging.
  - Les Houches angularity
  - number of sub-jets ( $k_T$ -algorithm,  $R = 0.2$  and  $p_T > 10$  GeV)
  - energy correlation functions.
  - Ratios of N-subjettiness (see later for definition)



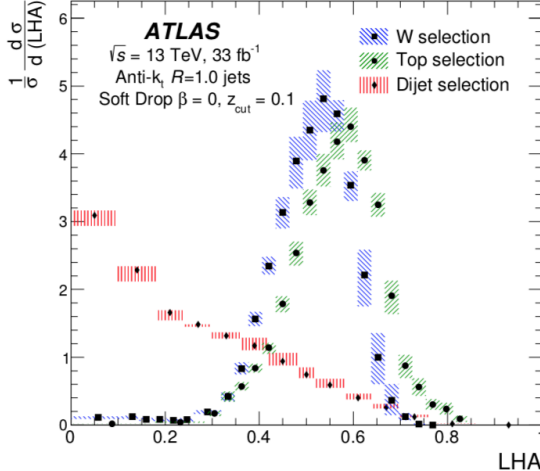
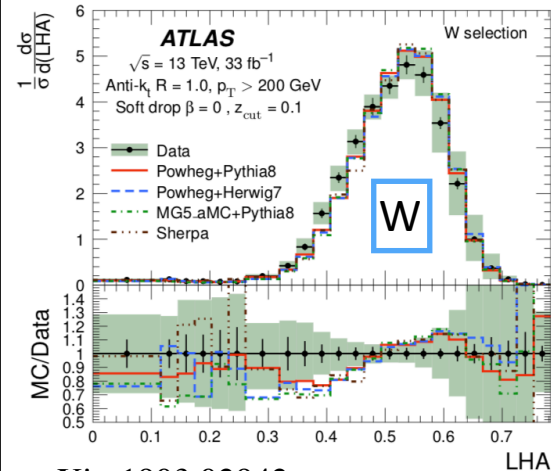
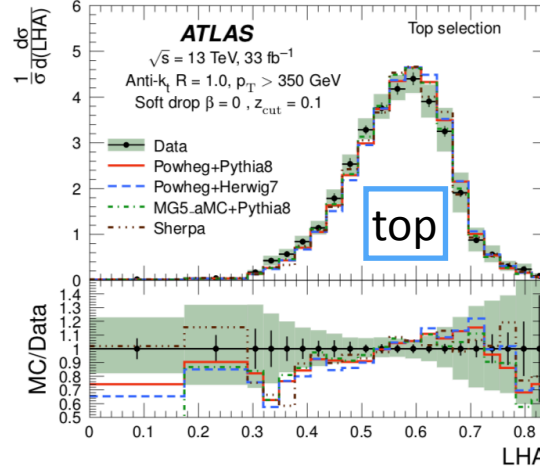
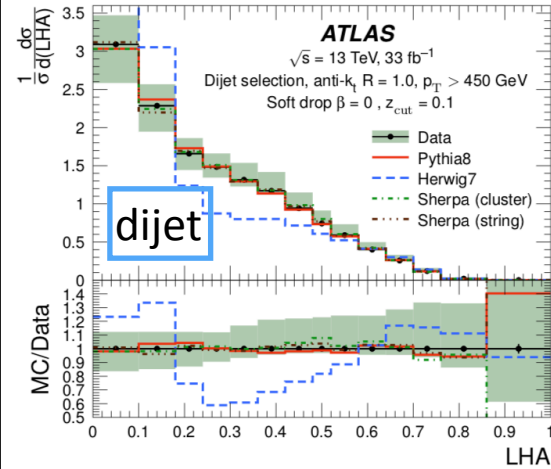
Good agreement for jet  $p_T$ . The discrepancy in the jet mass distributions is a known effect due to missing in-situ calibration and mass scale uncertainties.

$$\lambda_{\beta}^{\text{LHA}} = \sum_{i \in J} z_i^K \theta_i^{\beta \text{LHA}},$$

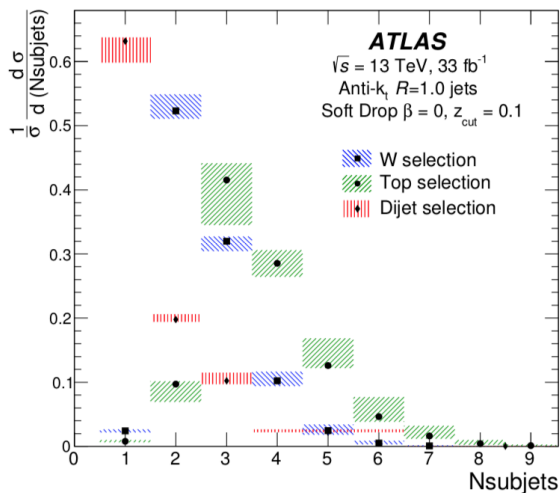
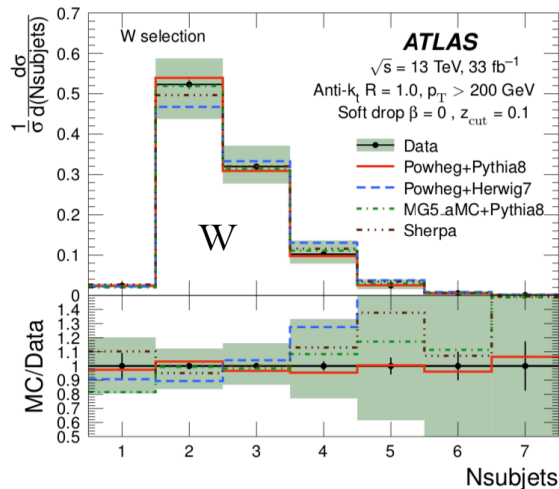
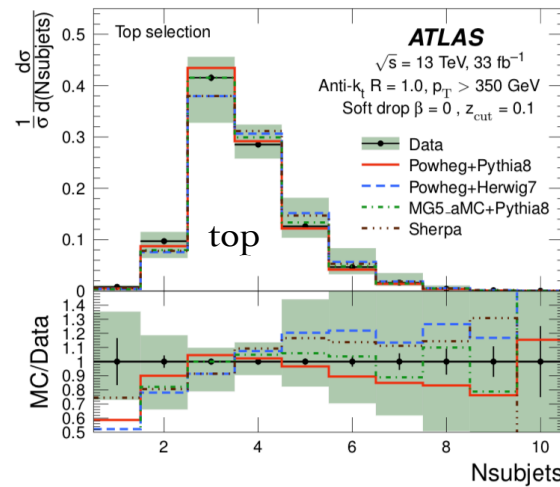
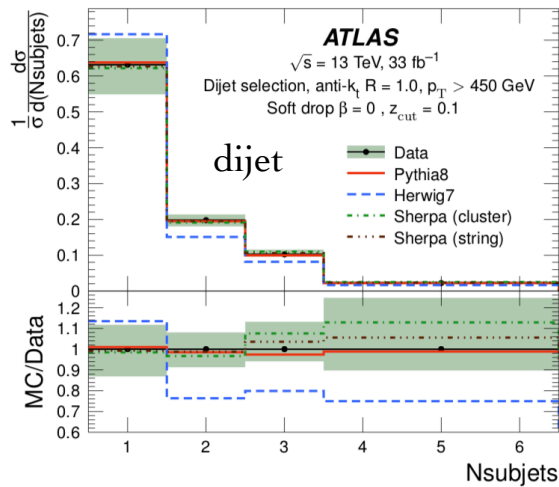
- where  $z_i$  is the transverse momentum fraction  $p_{T,i}/p_{T}^{\text{jet}}$
- $\theta_i$  is the angle of the constituent relative to the jet axis and  $\kappa = 1$  and  $\beta^{\text{LHA}} = 0.5$
- It is an infrared-safe version of the jet-shape angularity, and provides a measure of the broadness of a jet.

- discrepancies in generator predictions for top and W selections

- Dijets: good agreement except for Herwig 7.
- Good discrimination between q/g and W/top jets.



- number of sub-jets ( $k_T$ -algorithm,  $R = 0.2$  and  $p_T > 10$  GeV)



- Pythia8, Herwig7, Sherpa and MadGraph.
- Dijets: good agreement except for Herwig 7.
- W and top samples show good agreement for all generators.
- Largest contribution to uncertainties from mass and jet  $p_T$  calibration as well as calorimeter cluster corrections.
- Good discrimination between samples.

$$\text{ECF1} = \sum_{i \in J} p_{T_i}, \quad (\text{jet } p_T)$$

$$\text{ECF2}(\beta^{\text{ECF}}) = \sum_{i < j \in J} p_{T_i} p_{T_j} (\Delta R_{ij})^{\beta^{\text{ECF}}}, \quad (\text{jet mass})$$

$$\text{ECF3}(\beta^{\text{ECF}}) = \sum_{i < j < k \in J} p_{T_i} p_{T_j} p_{T_k} (\Delta R_{ij} \Delta R_{ik} \Delta R_{jk})^{\beta^{\text{ECF}}},$$

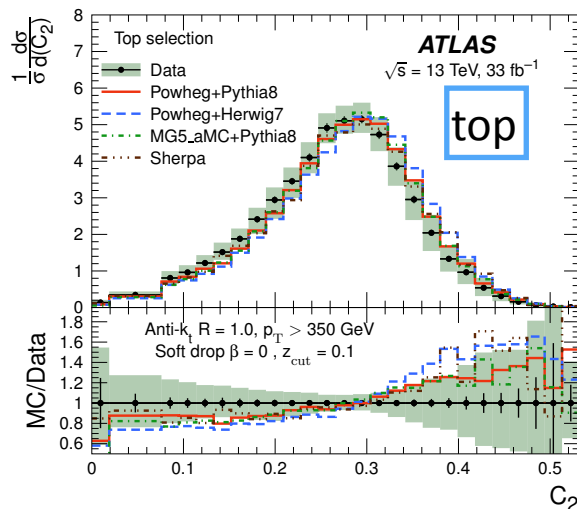
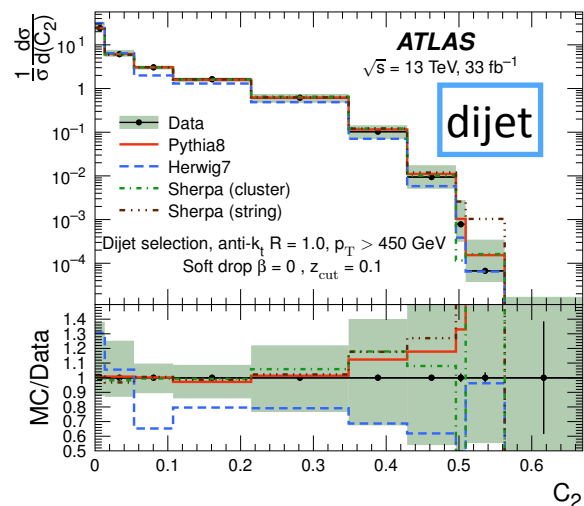
- Use  $\beta^{\text{ECF}}=1$  for this analysis and use the correlation functions in ratios:

$$e_2 = \frac{\text{ECF2}}{(\text{ECF1})^2}, \quad C_2 = \frac{e_3}{(e_2)^2},$$

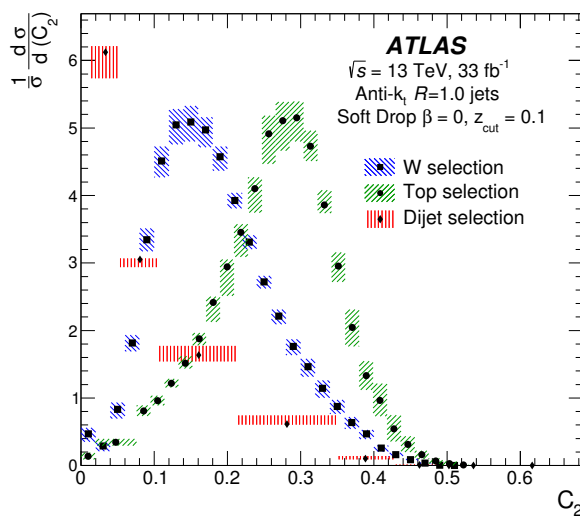
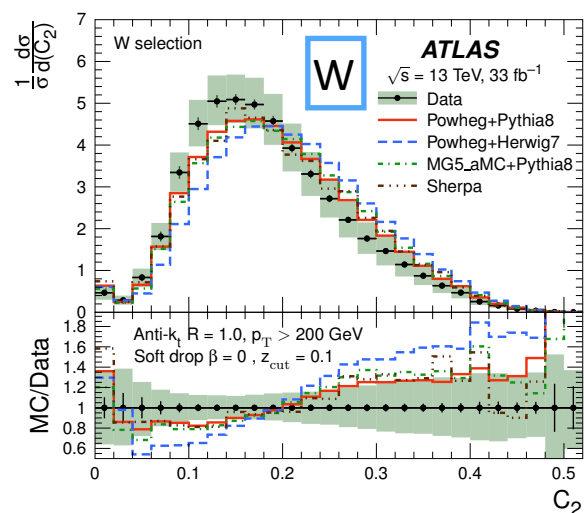
to form

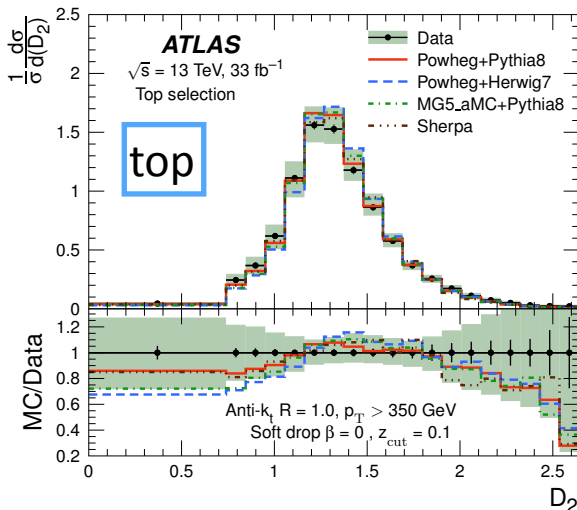
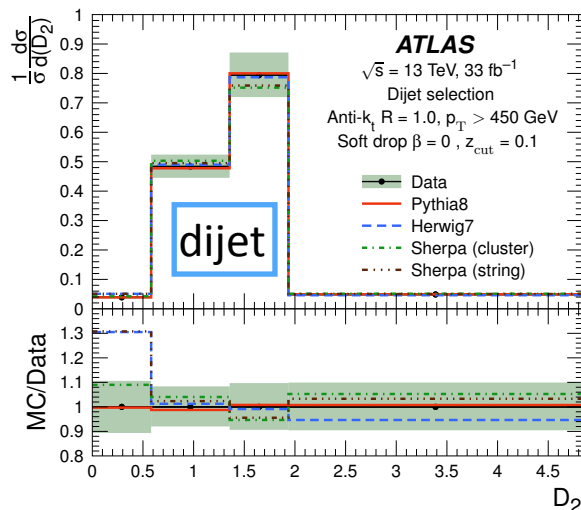
$$e_3 = \frac{\text{ECF3}}{(\text{ECF1})^3}, \quad D_2 = \frac{e_3}{(e_2)^3}.$$

- which are useful for identifying two-body structures within jets..

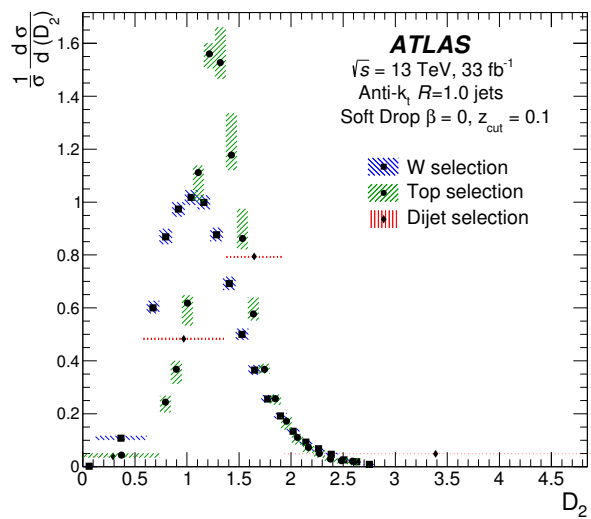
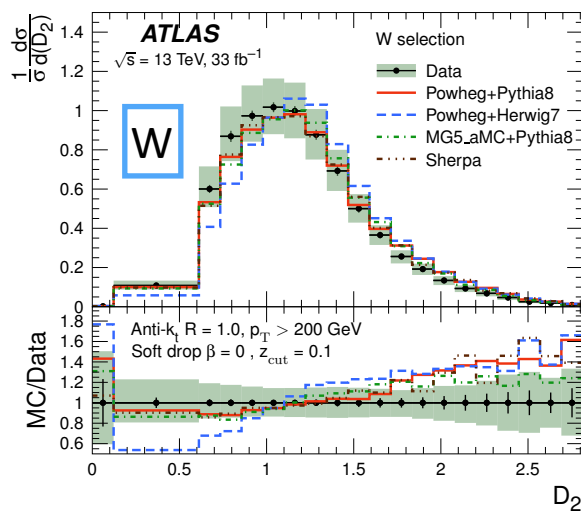


- Useful in W/top tagging
- Largest discrepancy for W-dataset.
- Excellent separation between q/g, W and top events.





- Useful in W/top tagging
- Largest discrepancy for W-dataset.
- Good separation between q/g, W and top events.





- N-subjettiness describes to what degree the substructure of a given jet is compatible with being composed of N or fewer objects

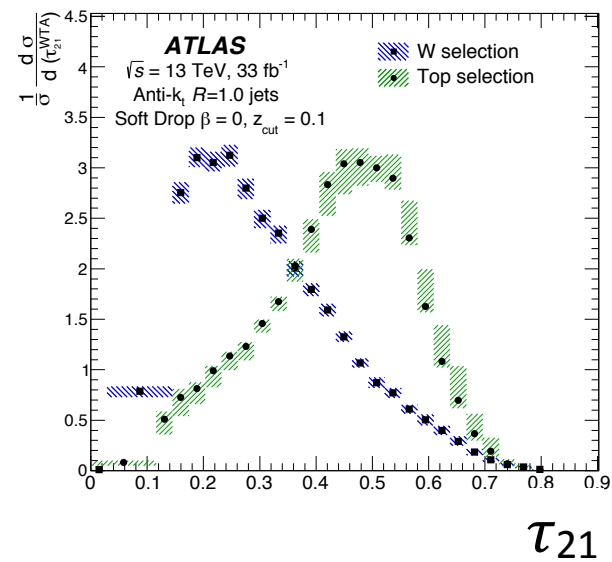
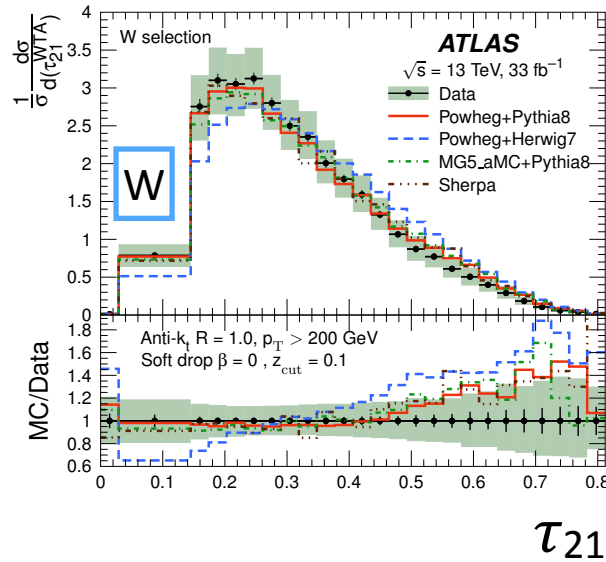
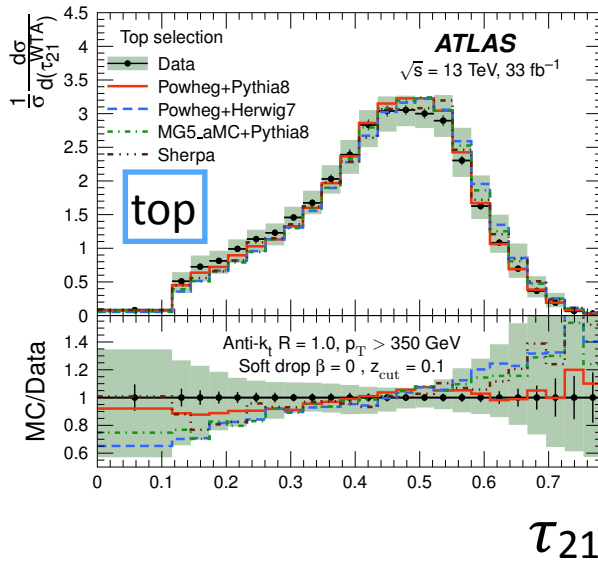
$$\tau_0(\beta^{\text{NS}}) = \sum_{i \in J} p_{T_i} R^{\beta^{\text{NS}}},$$

$$\tau_1(\beta^{\text{NS}}) = \frac{1}{\tau_0(\beta^{\text{NS}})} \sum_{i \in J} p_{T_i} \Delta R_{a_1, i}^{\beta^{\text{NS}}},$$

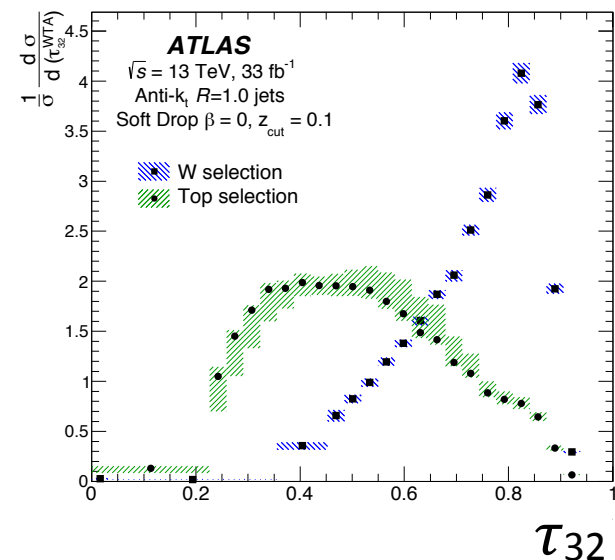
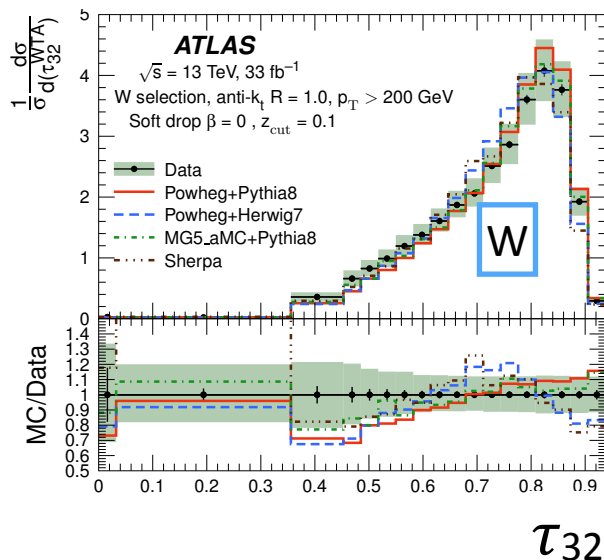
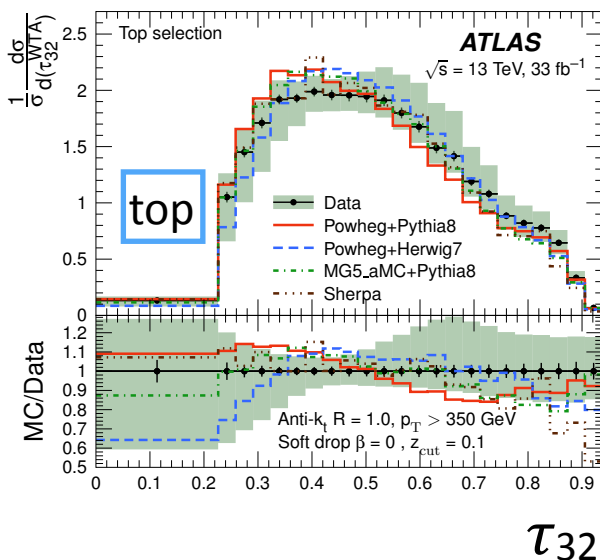
$$\tau_2(\beta^{\text{NS}}) = \frac{1}{\tau_0(\beta^{\text{NS}})} \sum_{i \in J} p_{T_i} \min(\Delta R_{a_1, i}^{\beta^{\text{NS}}}, \Delta R_{a_2, i}^{\beta^{\text{NS}}}),$$

$$\tau_3(\beta^{\text{NS}}) = \frac{1}{\tau_0(\beta^{\text{NS}})} \sum_{i \in J} p_{T_i} \min(\Delta R_{a_1, i}^{\beta^{\text{NS}}}, \Delta R_{a_2, i}^{\beta^{\text{NS}}}, \Delta R_{a_3, i}^{\beta^{\text{NS}}}),$$

- R is the radius parameter of the jet,  
 $\beta^{\text{NS}}=1$  is the angular separation weight  
 $\Delta R_{a,n}$  is the angular distance between constituent i and the axis of the n<sup>th</sup> subjet
- The ratios:  $\tau_{21} = \tau_2/\tau_1$  and  $\tau_{32} = \tau_3/\tau_2$  are useful in identifying two- and three-body structures in jets.
- Calculated using the direction of the hardest constituent in the subjet (WTA)



- Used in the top/W taggers
  - larger discrepancies for the W selection
  - Excellent discrimination between W and top events
- Not used on the dijet sample as these events have less hard splitting and are highly sensitive to the splitting and merging of clusters.



- Used in the top/W taggers
  - larger discrepancies for the W selection
  - Excellent discrimination between W and top events
- Not used on the dijet sample as these events have less hard splitting and are highly sensitive to the splitting and merging of clusters.

- jet substructure observables are widely used for W/top/H tagging in BSM searches
  - used in cut-based and multivariate taggers
- jet substructure uncertainties are of the order of 10 to 20% and allows
  - small enough to differentiate between the various MC models
- soft-drop groomer allows a comparison to NLO+NNL and LO+NNNL predictions
  - important to probe a new regime of QCD at LHC
  - improve the understanding of jet substructure properties
- dedicated measurements validate MC models, also show larger discrepancies for some observables
  - results can be used to tune MC generators!

# Backup

- *Measurement of jet-substructure observables in top quark,  $W$  boson and light jet production in proton-proton collisions at  $\sqrt{s}=13$  TeV with the ATLAS detector, [arXiv:1903.02942](#), submitted to JHEP, ([Link to ATLAS Repository](#)).*
- *A measurement of the soft-drop jet mass in  $pp$  collisions at  $\sqrt{s}=13$  TeV with the ATLAS detector, [Phys. Rev. Lett. 121 \(2018\) 092001](#), ([Link to ATLAS Repository](#)).*
- *In situ calibration of large- $R$  jet energy and mass in 13 TeV proton-proton collisions with the ATLAS detector, [Eur. Phys. J. C 79 \(2019\) 135](#), ([Link to ATLAS Repository](#)).*
- *A measurement of the soft-drop jet mass in  $pp$  collisions at  $\sqrt{s}=13$  TeV with the ATLAS detector, [Phys. Rev. Lett. 121 \(2018\) 092001](#), ([Link to ATLAS Repository](#)).*

jet constituents

jets

Simulated particles

Jet finding

Truth jets

Tracks

Jet finding

Track jets

Calorimeter clusters (EM scale)

Jet finding

Calorimeter jets (EM scale)

Local cluster weighting

Calorimeter clusters (LCW scale)

Jet finding

Calorimeter jets (LCW scale)

Calibrates clusters based on cluster properties related to shower development

## Dijets

	Detector level	Particle level
Dijet selection:		
Two trimmed anti- $k_t$ $R = 1.0$ jets	$p_T > 200$ GeV $ \eta  < 2.5$	$p_T > 200$ GeV $ \eta  < 2.5$
Leading- $p_T$ trimmed anti- $k_t$ $R = 1.0$ jet	$p_T > 450$ GeV	

Top and  $W$  selections:

Exactly one muon	$p_T > 30$ GeV $ \eta  < 2.5$ $ z_0 \sin(\theta)  < 0.5$ mm and $ d_0/\sigma(d_0)  < 3$	$p_T > 30$ GeV $ \eta  < 2.5$
Anti- $k_t$ $R = 0.4$ jets	$p_T > 25$ GeV $ \eta  < 4.4$ JVT output $> 0.5$ (if $p_T < 60$ GeV)	$p_T > 25$ GeV $ \eta  < 4.4$
Muon isolation criteria	If $\Delta R(\mu, \text{jet}) < 0.04 + 10 \text{ GeV} / p_{T,\mu}$ : muon is removed, so the event is discarded	None
$E_T^{\text{miss}}, m_T^W$	$E_T^{\text{miss}} > 20$ GeV, $E_T^{\text{miss}} + m_T^W > 60$ GeV	
Leptonic top	At least one small-radius jet with $0.4 < \Delta R(\mu, \text{jet}) < 1.5$	

Top selection:

Leading- $p_T$ trimmed anti- $k_t$ $R = 1.0$ jet	$ \eta  < 1.5$ , $p_T > 350$ GeV, mass $> 140$ GeV $\Delta R(\text{large-radius jet}, b\text{-tagged jet}) < 1$ $\Delta\phi(\mu, \text{large-radius jet}) > 2.3$
--	--

$W$  selection:

Leading- $p_T$ trimmed anti- $k_t$ $R = 1.0$ jet	$ \eta  < 1.5$ , $p_T > 200$ GeV, mass $> 60$ GeV and mass $< 100$ GeV $1 < \Delta R(\text{large-radius jet}, b\text{-tagged jet}) < 1.8$ $\Delta\phi(\mu, \text{large-radius jet}) > 2.3$
--	--

## hadronic top

## hadronic $W$



Process	Generator	Version	PDF	Tune	Use
Dijet	PYTHIA8	8.186	NNPDF23LO	A14	Nominal for unfolding
	SHERPA	2.2.1	CT10	Default	Validation of unfolding (with two different hadronisation models)
	HERWIG7	7.0.4	MMHT2014	H7UE	Comparison
$t\bar{t}$	POWHEG	v2	NNPDF30NLO		Nominal for unfolding
	+ PYTHIA8	8.186	NNPDF23LO	A14	
	POWHEG	v2	CT10		Validation of unfolding
	+HERWIG++	2.7	CTEQ6L1	UE-EE-5 tune	
	POWHEG	v2	CT10		Comparison
	+HERWIG7	7.0.4	MMHT2014	H7UE	
	MG5_aMC@NLO	2.6.0	NNPDF30NLO		Comparison
	+ PYTHIA8	8.186	NNPDF23LO	A14	
Single top	SHERPA	2.2.1	CT10	Default	Comparison
	POWHEG	v1	CT10		Nominal for unfolding
	+ PYTHIA6	6.428	CTEQ6L1	Perugia2012	
Z+jets	SHERPA	2.2.1	CT10	Default	Background estimation
W+jets	SHERPA	2.2.1	CT10	Default	Background estimation (nominal)
W+jets	MG5_aMC@NLO	2.2.5	CT10		Background estimation (cross-check)
	+ PYTHIA8	8.186	NNPDF23LO	A14	
Diboson	SHERPA	2.2.1	CT10	Default	Background estimation

- Default grooming procedure: trimming, removes  $R = 0.2$  subjects with  $p_T < 5\%$  of jet  $p_T$

